Journal of Magnetic Resonance **138,** 244–255 (1999)
Article ID jmre.1999.1733, available online at http://www.idealibrary.com on IDEAL®

Superslow Backbone Protein Dynamics as Studied by 1D Solid-State MAS Exchange NMR Spectroscopy

A. Krushelnitsky,* D. Reichert,† G. Hempel,† V. Fedotov,* H. Schneider,† L. Yagodina,* and A. Schulga‡

Kazan Institute of Biochemistry and Biophysics, Russian Academy of Sciences, Kazan, Russia; †Physics Department, Halle University, Halle, Germany; and ‡Institute of Bioorganic Chemistry, Russian Academy of Sciences, Moscow, Russia

Received October 21, 1998; revised February 2, 1999

Superslow backbone dynamics of the protein barstar and the polypeptide polyglycine was studied by means of a solid-state MAS 1D exchange NMR method (time-reverse ODESSA) that can detect reorientation of nuclei carrying anisotropic chemical shift tensors. Experiments were performed on carbonyl ^{13}C in polyglycine (natural abundance) and backbone ^{15}N nuclei in uniformly ^{15}N-enriched barstar within a wide range of temperatures in dry and wet powders for both samples. Two exchange processes were observed in the experiments: molecular reorientation and spin diffusion. Experimental conditions that are necessary to separate these two processes are discussed on a quantitative level. It was revealed that the wet protein undergoes molecular motion in the millisecond range of correlation times, whereas in dry protein and polyglycine molecular reorientations could not be detected. The correlation time of the motion in the wet barstar at room temperature is 50–100 ms; the activation energy is about 80 kJ/mol. Previously, protein motions with such a long correlation time could be observed only by methods detecting chemical exchange in solution (e.g., hydrogen exchange). The application of solid-state MAS exchange spectroscopy provides new opportunities in studying slow biomolecular dynamics that is important for the biological function of proteins.

Key Words: **protein dynamics; exchange NMR; spin diffusion; barstar; polyglycine.**

INTRODUCTION

NMR relaxation is presently the most powerful and informative tool for studying protein dynamics. During the past decade the most impressive achievements in this field have used multidimensional heteronuclear NMR spectroscopy in solution; see, for example, Refs. (*1–5*). The number of works dealing with solid-state studies is much smaller, primarily because of the lack of spectral resolution and hence selectivity of the dynamic information. However, solid-state experiments enable one to investigate the complete range of correlation times of the internal protein dynamics down to the millisecond–second range, whereas the solution NMR relaxation data provide information only about fast motions having correlation times shorter than that of the Brownian tumbling as a whole. This is so because the isotropic Brownian tumbling overlaps all slower protein motions, and thus the latter could not be detected in a liquid state relaxation experiment. In addition, it is well known that solution NMR techniques are not applicable for heavy (>50 kDa) and membrane proteins.

It has been shown by a variety of methods that internal protein dynamics spans a very wide range of frequencies. Unfortunately, by using measurements of standard relaxation parameters T_1, T_2, $T_{1\rho}$, or T_{1d}, even in the solid state one may obtain information only about molecular motions in the pico-, nano-, and microsecond range of correlation times, and slower protein motions are not accessible by use of those techniques (*6–12*). On the other hand, it is intuitively clear that slow and large-scale protein dynamics can be important for protein function and thus, studying it is very interesting from the biological point of view. For this, other NMR techniques are necessary.

Solid-state exchange NMR spectroscopy is just one of the methods that enable study of very slow molecular motions (*13*). It can detect reorientations of magnetic nuclei carrying anisotropic chemical shift tensors. In proteins, backbone nitrogens and carbonyl carbons are very convenient for performing exchange experiments because unlike the side-chain atoms, those types of nuclei have rather anisotropic chemical shift tensors. It is commonly believed that the upper limit of the correlation times of the molecular motions that can be studied by use of this method is the value of T_1 which can be of the order of tens of seconds in solids. Thus, this kind of experiment represents a unique possibility for studying superslow molecular dynamics.

It is well known that many proteins reveal internal flexibility on a slow time scale. For instance, it was shown that in barstar (this protein is being studied in the present work) a significant number of residues undergo slow conformational exchange (*14*). However, up to now the information about slow internal protein motions could be only obtained with the help of methods detecting chemical exchange in solution, such as hydrogen exchange, aromatic ring flips, T_2 shortening, $T_{1\rho}$ vs B_1 field dependence, and some others

1090-7807/99 $30.00

(*15–18*). Yet these methods are able to define the frequency and activation energy of slow protein motions at best, but studying the amplitude or molecular models of the motion is much more complicated, if possible at all, in comparison with the relaxation NMR techniques.

Unlike the case in solution, in the solid state the chemical shift anisotropy is not averaged out by the fast Brownian tumbling, and that is why solid state exchange experiments permit investigation of both frequency and amplitude parameters on a more detailed level. In spite of this, to our knowledge exchange NMR spectroscopy was not applied for protein dynamics investigations so far. The main reason for this might be the low signal/noise ratio and long experimental time necessary for performing two-dimensional exchange experiments of a reasonable quality. Recently, one-dimensional modifications of the exchange experiment have become available. The most recent one, so-called time-reverse ODESSA (*19*), provides the same dynamic information as 2D MAS exchange experiments but reduces the experimental time by at least one order of magnitude. This paper presents first results of the application of one-dimensional exchange techniques for studying protein backbone dynamics in the solid state.

In this work we performed the NMR experiments on a uniformly enriched protein, and thus we could characterize the protein by averaged parameters only. From the point of view of studying the specific protein, using selective labeling would be of course more interesting, but the lower signal-to-noise ratio that we would get with selective labeling would not allow us to perform the extensive set of measurements at different temperatures and moistures within a reasonable time. In addition, preparing the selectively labeled protein is much more complex and time consuming. Our main goal was to define whether the 1D exchange method can detect slow molecular motion in proteins at all, and if so, to determine the parameters of this motion and the optimal experimental conditions for its investigation. After these questions are answered, additional techniques should be applied to obtain high-resolution NMR spectra; this will be a subject for future studies.

EXPERIMENTAL

Samples

In the present work two samples were studied—natural abundance polyglycine and totally ^{15}N enriched protein barstar. Polyglycine (M_w 5000–10,000) was purchased from Sigma and used without additional purification. According to IR-spectroscopy data, the polyglycine was primarily in β-sheet conformation.

Barstar is the 89-residue polypeptide inhibitor of RNase from *Bacillus amyloliquenfaciens.* The same organism produces extracellular endoribonuclease barnase. Barstar interacts with barnase with a dissociation constant of 2×10^{-14} M and inhibits its lethal RNase activity inside the cell. The interaction between barstar and barnase is known as one of the fastest and tightest protein–protein interactions. We selected barstar for our experiments for two reasons. First, the biochemical properties and spatial structure of this protein are well known (*20–23*). Second, barstar can serve as a very convenient model system for studying interconnection of protein dynamics and interprotein interactions in future studies. However, we must admit that for this work, at the present stage of our investigations, the protein used was not a critical issue.

To prepare ^{15}N labeled barstar we used the laboratory method of overexpression in the pET system that was worked out by one of the authors (A.S.). The T7 RNA polymerase system is one of the most widely used for bacterially expressed proteins (*24, 25*). In this system the gene encoding the protein of interest is placed under the control of the T7 promoter, which is recognized as a translation start site by the RNA polymerase from phage T7 but not by the RNA polymerase of host *Escherichia coli.* The gene encoding the barstar was placed behind a T7 RNA polymerase promoter in pGEMEX-1 (Promega, USA) plasmid vector that also confers ampicillin resistance (*26*). The pGEMEX-1 vector was used to transform BL21(DE3) cells that carry the gene for T7 RNA polymerase under an IPTG-inducible promoter.

Colonies were grown overnight in LB broth containing 50 mg/L ampicillin at 37°C (*27*). The cells were grown on a M 9 minimal medium (*27*) with [^{15}N]ammonium chloride (200 mg/L) as the only nitrogen source. The cell pellet was resuspended in buffer A: 50 mM Tris-HCl with 1 mM phenylmethanesulfonyl fluoride, 2 mM dithiothreitol, 1 mM sodium azide, pH 8.0. The solution was sonicated and centrifuged in a K-24 (20 min, 9000 rpm). The proteins in the supernatant were precipitated with 40–80% ammonium sulfate. The fraction of 80% ammonium sulfate was centrifuged (K-24, 30 min, 10,000 rpm) and the pellet was dissolved in a minimal volume of buffer A. The resulting solution was loaded on a Pharmacia Sephadex G-75 column and eluted at a flow rate of 0.2 ml/min using the same buffer. Column fractions were combined for an ion-exchange step using a Pharmacia Mono-Q 10/10 column equilibrated in 50 mM Tris-HCl, pH 8 (*23*). The resulting peak of labeled ^{15}N-barstar was a single band when analyzed by SDS–PAGE. The protein was lyophilized and stored at −20°C. The amount of the sample used in the present work was 65 mg.

For experiments we used dry and wet powders. The first one was dried under vacuum at room temperature during one day. The wet samples (0.2 g H_2O per g of dry protein/polypeptide) were prepared in a vacuum exsicator. Amount of water in the samples was defined gravimetrically.

NMR Experiments

MAS experiments were performed using a INOVA400 spectrometer and a VARIAN 7mm VT-CPMAS probe, operating at 100.55 MHz for ^{13}C and 40.51 MHz for ^{15}N, respectively. Both MAS spinning rate and temperature were controlled by the spectrometer; their stability was better than 1 Hz and 1 K, respectively. Typical length of $\pi/2$ pulses was about 5 μs both for ^{13}C and ^{15}N experiments. Constant amplitude cross-polarization was applied with the frequency 50 kHz for both types of nuclei under conditions $\omega_{1H} = \omega_{13C}$ and $\omega_{1H} = \omega_{15N}$. Contact times were 0.5–1.5 ms. Repetition times were 1–8 s depending on the sample and temperature. The experiments were performed within a wide range of temperatures. At each temperature, T_1 and MAS exchange (time reverse ODESSA) decays were measured. Time-reverse ODESSA experiments were performed as described in detail in Ref. (*19*). This experiment is a 1D-exchange experiment based on the rotor-synchronized 2D MAS exchange experiment as described in Ref. (*28*): after cross-polarization, a delay of half of a rotor cycle ($T_R/2$) follows. A $\pi/2$ pulse takes the magnetization into the z direction, where during a rotor-synchronized mixing time $\tau_m = (N - \frac{1}{2}) \cdot T_R$, the exchange (either molecular reorientation or spin exchange, see below) is allowed to take place. A final $\pi/2$ pulse takes the magnetization back to the x–y-plane, where after another delay of $T_R/2$, the FID is recorded under CW ^1H decoupling at 75 kHz. Proper phase cycling was applied to achieve the correct combination of the sine and the cosine experiments as well as to suppress axial magnetization. The theory of the method with emphasis on our experiments is recalled briefly in the next section. Longitudinal relaxation times T_1 were measured according to the method proposed by D. Torchia (*29*). Chemical shifts were defined in respect to glycine for ^{13}C (43 and 176.1 ppm) and nitromethane CH_3NO_2 for ^{15}N (0 ppm).

THEORY

In the time-reverse ODESSA experiment the information about the dynamic process can be extracted from the intensities of the spinning sidebands depending on mixing time τ_m (ODESSA decay):

$$I^N(\tau_m) = \sum_{i,j} P_{ij}(\tau_m) \cdot \sum_M (-1)^{M+N} I_{ij}^{MN}. \qquad [1]$$

$P_{ij}(\tau_m)$ is the probability of finding a nucleus at time τ_m at site j when it was at site i at time 0. I_{ij}^{MN} are the 2D MAS subspectra for the exchange between site i and j (M,N are the numbers of spinning sidebands in the two dimensions; $M = N = 0$ corresponds to the isotropic line). For all i and j it is always true that $I_{ij} = I_{ji}$. Although $P_{ij}(\tau_m)$ contains the information about the time scale of the dynamic process and the pathway of the exchange (see below), I_{ij}^{MN} carries the information about the geometrical model of the dynamics, i.e., jump angles and number of sites. The latter depends on the CSA tensor elements, the MAS spin rate, and the Euler angles defining the mutual orientation of the CSA tensors at the exchanging sites, and it must be calculated numerically (*19, 28*). Actually, the exchange process can be caused by molecular reorientation (MR) of a nucleus having an anisotropic chemical shift tensor, or by spin exchange (SE) between different nuclei (commonly termed spin diffusion; here we imply no difference between spin exchange and spin diffusion), or by both. In the first case sites i and j (Eq. [1]) correspond to different orientations of the same nuclei, and in the second case these sites correspond to different nuclei.

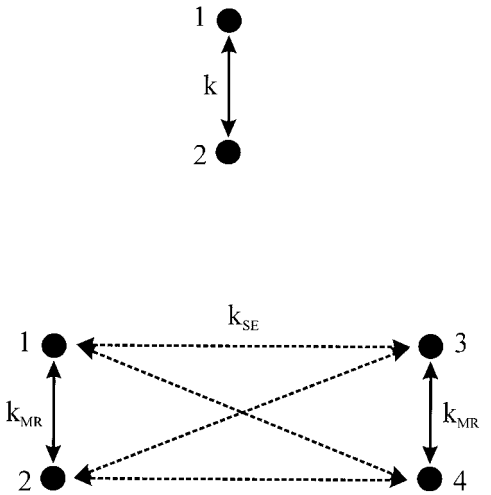

FIG. 1. Two- and four-site models of the exchange. In the latter case sites 1 and 2 belong to the first nucleus, and sites 3 and 4 belong to the second. The exchange between sites 1 and 2 is the result of the molecular reorientation, as well as the exchange between sites 3 and 4. The exchange pathways marked by dashed arrows correspond to the spin exchange between two nuclei.

$P_{ij}(\tau_m)$ can be calculated by solving (*30*)

$$P_{ij}(\tau_m) = (e^{\mathbf{K}\cdot\tau_m})_{ij} \cdot P_j(0). \qquad [2]$$

$\mathbf{K}$ is the exchange matrix with elements k_{ij} (k_{ij} is the probability of a nucleus changing from site j to site i) and $P_j(0)$ is the equilibrium populations of the exchanging sites. Assuming a simple symmetric two-site exchange process with a single jump rate k between the sites (Fig. 1, top), a site population of $P(0) = \frac{1}{2}$, and a spin–lattice relaxation time T_1 being equal for both sites, the exchange matrix $\mathbf{K}$ can be written as

$$\mathbf{K} = \begin{pmatrix} -k - \dfrac{1}{T_1} & k \\ k & -k - \dfrac{1}{T_1} \end{pmatrix}. \qquad [3]$$

Solving [2], one easily obtains

$$\mathrm{P}_{ij}(\tau_\mathrm{m}) = \frac{1}{4}\, e^{-(\tau_\mathrm{m}/T_1)} \begin{pmatrix} 1 + e^{-2k\tau_\mathrm{m}} & 1 - e^{-2k\tau_\mathrm{m}} \\ 1 - e^{-2k\tau_\mathrm{m}} & 1 + e^{-2k\tau_\mathrm{m}} \end{pmatrix}, \qquad [4]$$

resulting in the ODESSA decay

$$\frac{I^N(\tau_\mathrm{m})}{I^N(0)} = [1 - P_\mathrm{ex}(1 - e^{-(\tau_\mathrm{m}/\tau_\mathrm{ex})})] \cdot e^{-(\tau_\mathrm{m}/T_1)}\, I^N(0) = I^N_{11};$$

$$P_\mathrm{ex} = \frac{I^N_{11} - I^N_{12}}{2I^N_{11}}; \quad I^N_{ij} = \sum_M (-1)^{M+N} \cdot I^{MN}_{ij};\ \tau_\mathrm{ex} = \frac{1}{2k}. \qquad [5]$$

Equation [5] directly emphasizes the relative amplitude P_ex of the dynamic process on the overall ODESSA decay that we will call "exchange decay." The parameter P_ex has a certain connection with the order parameter S^2 that is widely used in NMR relaxation data analysis using the so-called model-free approach (*31*). In the case of molecular reorientation, both these parameters are measures of a motional amplitude, but they do not give information about the model of the motion. Both S^2 and P_ex have in common that to define the angle amplitude of the motion, one must first choose a model for that motion. However, S^2 depends on geometrical parameters only, characterized by topology of the molecular dynamics, whereas P_ex is a spectral parameter of the 2D MAS exchange experiment that is determined by the topology of the dynamics as well as by NMR parameters, namely the CSA-tensor elements and the MAS-spinning frequency. Thus, one might argue that P_ex depends on S^2 plus additional NMR parameters. However, the exact relation between them is complicated (although in principle known), and the calculation can be done only numerically. In turn, recalculating the S^2 from the experimentally obtained P_ex might be possible; however, it is not yet clear whether this will lead to unambiguous results. Consequently, we decided to use the well-defined P_ex for characterizing the relative amplitude of the molecular reorientation.

In simple molecules, the nature of the process might be obvious and only the exact jump angle is unknown. In these cases, detailed geometrical information of the process can be obtained from the experimentally accessible parameter P_ex. However, in more complicated systems, where neither the number of exchanging sites nor any information about the type of the process is available, one can only estimate the range at which the geometrical parameters (for example, jump angles) are compatible with the experimental result, as we will discuss below.

Equation [5] holds both for molecular reorientation and for spin exchange between two sites. In real systems, both processes might be present simultaneously. In cases where the geometry of the SE cannot be distinguished from that of the MR by the NMR experiment, i.e., the SE happens between the same sites as the MR, and the SE between more remote sites is negligible, Eq. [5] still holds, but with a modified jump rate

$$k = k_\mathrm{MR} + k_\mathrm{SE}, \qquad [6]$$

where k_MR and k_SE are the molecular reorientation and spin exchange rates, respectively.

However, in general case the geometry of the SE and MR processes might be different. The simplest example that is relevant for our case is the SE occurring between neighboring nuclei that undergo MR, as shown in Fig. 1 (bottom). In that case the exchange matrix becomes

$$\mathbf{K} = \begin{pmatrix} -2k_\mathrm{SE} - k_\mathrm{MR} - \frac{1}{T_1} & k_\mathrm{MR} & k_\mathrm{SE} & k_\mathrm{SE} \\ k_\mathrm{MR} & -2k_\mathrm{SE} - k_\mathrm{MR} - \frac{1}{T_1} & k_\mathrm{SE} & k_\mathrm{SE} \\ k_\mathrm{SE} & k_\mathrm{SE} & -2k_\mathrm{SE} - k_\mathrm{MR} - \frac{1}{T_1} & k_\mathrm{MR} \\ k_\mathrm{SE} & k_\mathrm{SE} & k_\mathrm{MR} & -2k_\mathrm{SE} - k_\mathrm{MR} - \frac{1}{T_1} \end{pmatrix}. \qquad [7]$$

For the small-amplitude molecular reorientation, it can be assumed that $I_{13} = I_{14} = I_{23} = I_{24}$. Also, for simplicity we assume that the amplitude and type of the molecular reorientation is the same for both nuclei, meaning that $I_{12} = I_{34}$. In this case the normalized ODESSA decay of the line intensity vs τ_m becomes

$$\frac{I^N(\tau_m)}{I^N(0)} = [1 - P_{ex1}(1 - e^{-(\tau_m/\tau_{ex1})}) - P_{ex2}(1 - e^{-(\tau_m/\tau_{ex2})})] \cdot e^{-(\tau_m/T_1)}$$

$$I^N(0) = I^N_{11}; \quad P_{ex1} = \frac{I^N_{11} - I^N_{12}}{2I^N_{11}};$$

$$P_{ex2} = \frac{I^N_{11} + I^N_{12} - 2I^N_{13}}{4I^N_{11}};$$

$$\tau_{ex1} = \frac{1}{2(k_{MR} + k_{SE})}; \quad \tau_{ex2} = \frac{1}{4k_{SE}}. \quad [8]$$

Note that k_{MR} must depend on temperature while k_{SE} does not, thus providing an opportunity to separate MR from SE. It is obvious from Eq. [8] that the molecular reorientation can be detected by the exchange experiment if and only if $k_{MR} > k_{SE}$. Otherwise, one would see only the SE and there would be no temperature dependence of the exchange decay components.

In general, because of the many-body nature of the spin exchange and its strong dependence on the distance between the exchanging nuclei, the ODESSA decay due to spin exchange must be described by a multiexponential rather than by a single exponential decay (*32, 33*). However, the analytical expression for the exchange decay in this case would be too complicated and the exchange decay can be simulated only numerically, as presented below.

RESULTS AND DISCUSSION

Analysis of the Shape of the Exchange Decays

In Figs. 2 and 3, CP/MAS spectra of dry barstar (^{15}N) and polyglycine (^{13}C) are shown, respectively. Since the relative amplitude of the exchange component of the decay in MAS exchange experiments strongly depends on the intensity of the sideband lines, it is desirable to get sideband lines as high as possible. Hence, one has to spin a sample rather slowly. On the other hand, slow spinning reduces the signal-to-noise ratio of the isotropic line. Thus, finding an optimal value of MAS rate is an important issue for the exchange experiments. Figure 2 represents the ^{15}N spectrum of barstar at 2 and 5 kHz MAS rates. The isotropic peak at about −261 ppm corresponds to the backbone nitrogens. In addition, there are two weak peaks at −309 and −348 ppm corresponding to the side-chain nitrogens contained in His, Arg, Lys, Gln, Asn, and Trp. The 5 kHz spinning provides a good signal-to-noise ratio and separation of all lines of the spectrum. However, the amplitude of the sideband lines is rather low, and we could not perform an accurate analysis of the short component of the exchange decay at this MAS rate. Spinning at 2 kHz reduces the signal-to-noise ratio and leads to the sideband and one of the side-chain lines overlapping at −309 ppm. However, in this case the relative

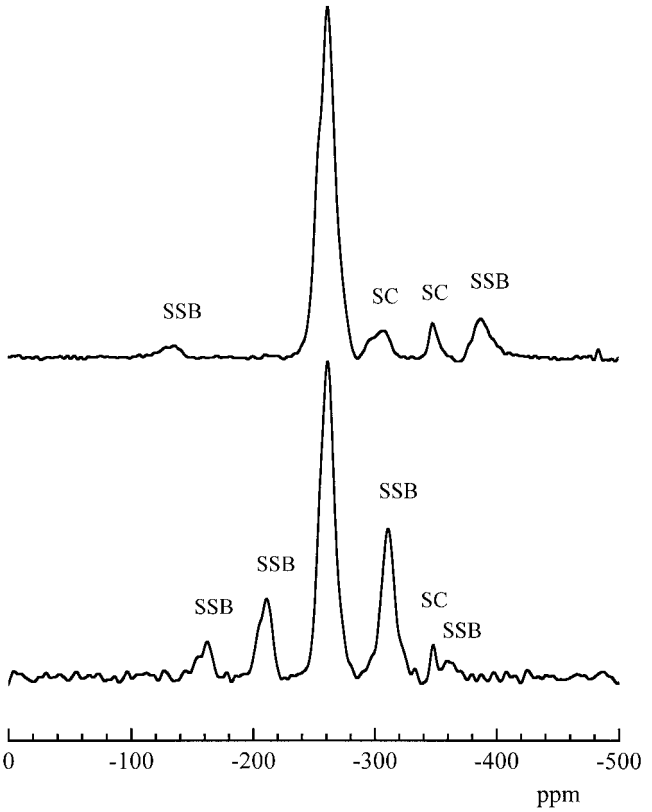

FIG. 2. ^{15}N CP/MAS spectra of the totally enriched barstar. MAS rate 2 kHz (bottom), 5 kHz (top). Room temperature, proton decoupling field 70 kHz. Denotations: SC, lines corresponding to side chain nitrogens; SSB, spinning sidebands.

amplitude of the exchange component of the decay is much higher, which permits more accurate treatment of the experiment. The natural-abundance ^{13}C spectrum of polyglycine contains only two lines corresponding to carbonyl C═O and CH_2 carbons. Spinning at 3 kHz seems to be optimal for the experiment. In both ^{13}C and ^{15}N experiments we analyzed the decays of the heights of the isotropic lines corresponding to carbonyl carbons and backbone nitrogens, respectively, since they have higher amplitudes in respect to the sideband lines.

We also attempted to perform the exchange experiments on natural-abundance ^{13}C nuclei in barstar. However, because of the wider lines in the protein, the signal-to-noise ratio was too poor to allow smooth decays to be obtained within the reasonable time limits. Figures 2 and 3 clearly demonstrate that only backbone nitrogens and carbonyl carbons have rather anisotropic chemical shift tensors that enable to perform exchange experiments. Unfortunately, side-chain atoms have less wide anisotropy of chemical shift tensors, and using them for this kind of experiments is practically impossible.

In Fig. 4, typical ^{13}C and ^{15}N exchange and T_1 decays are shown. The comparison of these two types of the experiment unambiguously tells us about an exchange process due to the

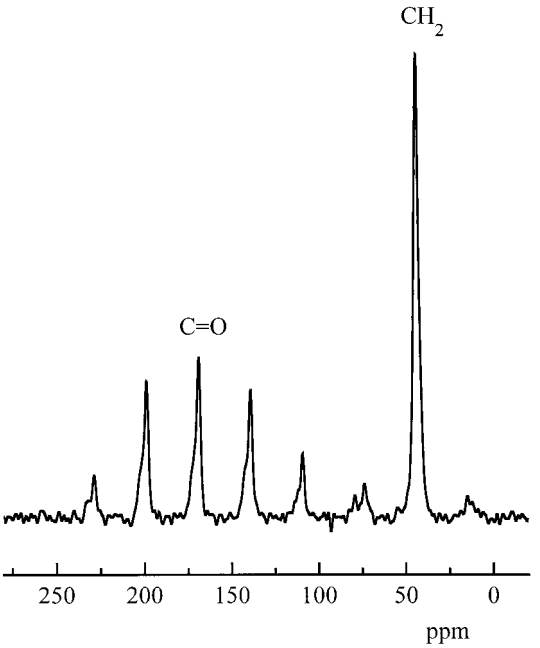

FIG. 3. ^{13}C natural abundance CP/MAS spectrum of polyglycine. Room temperature, MAS rate 3 kHz, proton decoupling field 70 kHz.

strong component of the exchange decays having a correlation time shorter than T_1. To define whether this process is an SE or MR or a combination of both, one needs to perform the exchange measurements at different temperatures. Special attention should be paid to the initial part of the decays, since according to Eq. [8], the variation of the correlation time of the molecular reorientation can be detected only if it is shorter than k_{SE}^{-1}.

In Figs. 5 and 6 the normalized ^{15}N exchange decays in wet and dry barstar at various temperatures are shown. In order to compare the exchange decays measured at different temperatures for dry and wet sample directly, they were divided by the experimentally obtained T_1 decays. From Fig. 4 it can be seen that the T_1 decay is very close to an exponential. However, more accurate analysis revealed a small deviation of the shape of the T_1 decay from an exponential. Although it was not of principal importance, we approximated all T_1 decays as biexponentials, and that approximation was used while dividing the exchange decays. In this way we eliminated the influence of the dependence of T_1 on temperature and humidity of the sample, and thus the exchange decays measured at different conditions can be compared directly.

From Fig. 5 it can be seen that at higher temperatures ($T > 0°C$) the initial part of the exchange decays strongly depends on temperature, while at mixing times longer than 0.5 s, all decays overlap (Fig. 5, left). On the other hand, at lower temperatures there is no temperature dependence of the exchange decays in the wet sample at all (Fig. 5, right). Such behavior is in complete correspondence with Eq. [8]: In the wet protein there are two exchange processes—MR and SE. At $T > 0°C$, $k_{MR} > k_{SE}$ is valid, and thus one may observe the temperature dependence of the exchange decays. At lower temperatures k_{MR} becomes less than k_{SE}; hence, the shape of the exchange decays is defined by spin exchange only (Eq. [8]), and no temperature dependence is detectable.

As shown from Fig. 6, there is no detectable temperature dependence of the exchange decays in the dry protein at all temperature ranges. That means either the correlation time of the molecular motion is too slow so that at all temperatures $k_{MR} < k_{SE}$ is valid, or the amplitude of the molecular motion in the dry protein becomes too little so that it cannot be seen in the experiment. Our data do not provide the possibility of making an unambiguous choice between these two options; however, the latter seems to us more reasonable since we do not observe any changes within a very wide range of temperatures.

Exchange decays in polyglycine samples are shown in Fig. 7. In this case we did not divide them by longitudinal relaxation decays, since T_1 of carbonyl carbons in polyglycine is very long (about 100–150 s) and practically does not depend on temperature and humidity of the sample. It is shown that within the experimental error both dry and wet samples do not reveal any temperature dependence. That means that the exchange process seen in

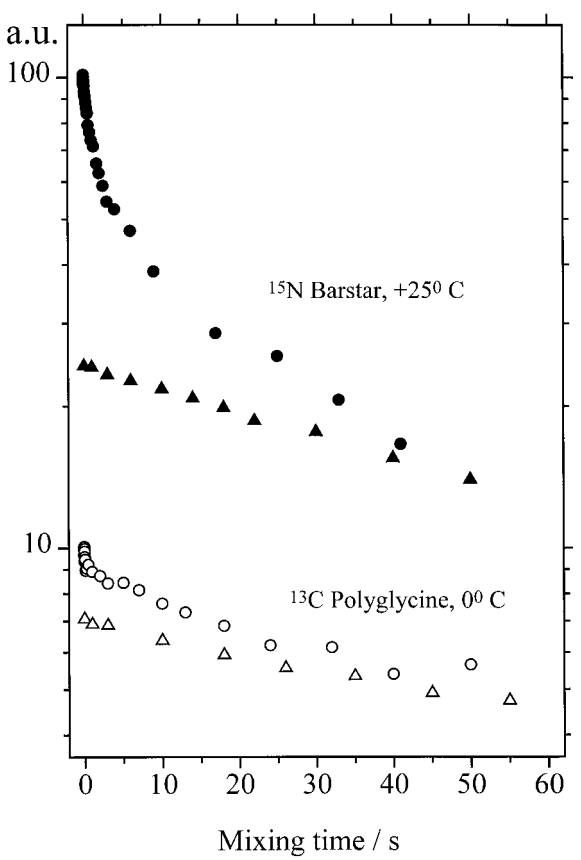

FIG. 4. Typical examples of the exchange (circles) and T_1 (triangles) decays in dry barstar (solid symbols) and wet polyglycine (open symbols).

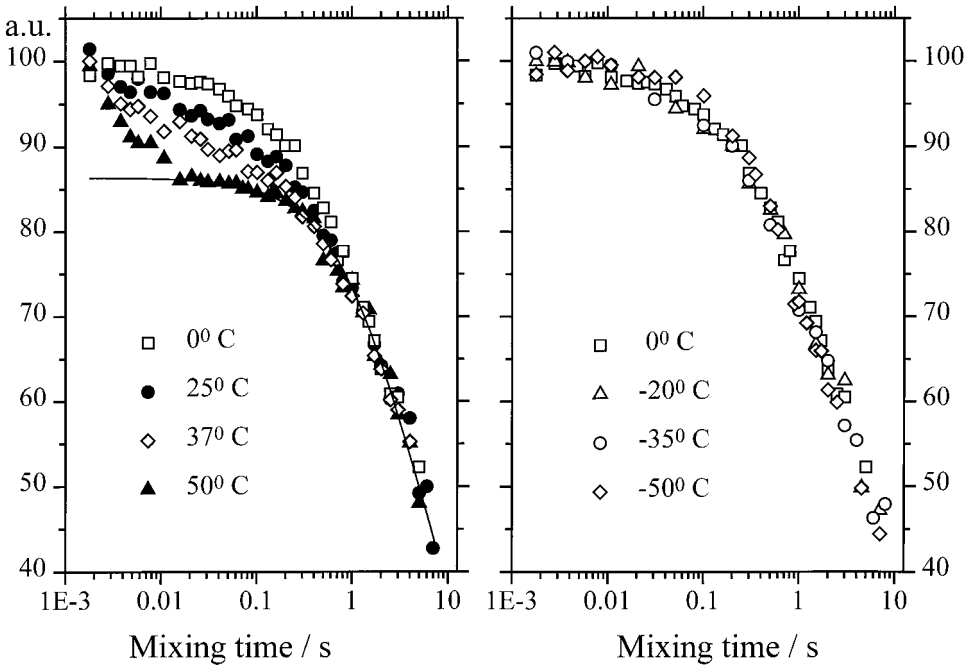

FIG. 5. ^{15}N exchange decays divided by T_1 decays (which were measured separately by the Torchia method) for wet barstar at different temperatures. The long-mixing-time parts of the exchange decays are not shown because of the relatively short T_1 in the wet sample. The solid lines on the left plot are the SE component obtained by biexponential approximation of the +50°C exchange decay at mixing times from 20 ms to 8 s.

polyglycine is solely due to the spin diffusion. A certain difference between dry and wet samples observed at longer mixing times (Fig. 7) can be ascribed, as we believe, to the slightly different packing density of the polypeptide chain: in wet polyglycine, water molecules are located between the peptide chains and the average distance between ^{13}C nuclei slightly increases. Since the spin diffusion rate is proportional to $1/r^6$ (see below), this slows down the spin diffusion process in the wet sample, as seen in Fig. 7.

Thus, from the qualitative analysis of the exchange decays one may conclude that in both samples at all conditions there is a strong component of the decays caused by spin diffusion. Molecular reorientation is seen only in the wet protein at high temperatures. These two exchange processes are analyzed quantitatively in the next sections.

Spin Exchange (Diffusion)

As mentioned above, the shape of the spin diffusion decay is defined by the distribution of internuclear distances in the molecule. We made an attempt to calculate the shape of the ^{15}N spin diffusion decay in barstar proceeding from the spatial structure of the protein. It is well known that the exchange rate between two nuclei is inversely proportional to the sixth power of the distance between them. Thus, we assume that the transition probability between two ^{15}N nuclei is

$$k_{ij} = \frac{A}{r_{ij}^6}, \qquad [9]$$

where A is a fitting parameter. It depends on a set of parameters of the spin system (*32*) that are not known *a priori.*

To calculate the exchange decay using Eq. [1], we need to know the 2D MAS exchange line intensity I_{ij}^{MN} values. As mentioned in the Theory section, I_{ij}^{MN} depends on MAS rate, diagonal CSA tensor elements σ_{xx}, σ_{yy}, σ_{zz}, and Euler angles α, β, γ, defining the relative orientation of site i with respect to site j. The MAS rate is a known parameter (2 kHz for ^{15}N experiments); the tensor elements can be found from the sideband line intensities of the CP/MAS spectrum using the Herzfeld–Berger procedure (*34*). We found parameters σ_{xx}, σ_{yy}, σ_{zz} to be 108, −30, −78 ppm and assumed identical CSA tensors for all nitrogens. The Euler angles can be computed from the known spatial structure of barstar (Brookhaven Protein Data Bank file 1BTA, (*23*)). Although it does not provide information about the chemical shift tensor of nitrogen nuclei, there are literature data on the orientation of the tensor axes with respect to the chemical bonds (*35*). According to this work, we oriented the x axis of the tensor along the N–C bond (where C is a carbonyl carbon of an antecedent aminoacid residue); the y axis was chosen to be perpendicular to the C–N–C_α plane, and orientation of the z axis is self-evident. It should be noted that we do not even need the absolute orientation of the tensor: Because of the powder averaging, we just need to know how two neighboring ^{15}N nuclei tensors are oriented with respect to each other, and it does not matter how these tensors are oriented with respect to the molecular frame, as long as we

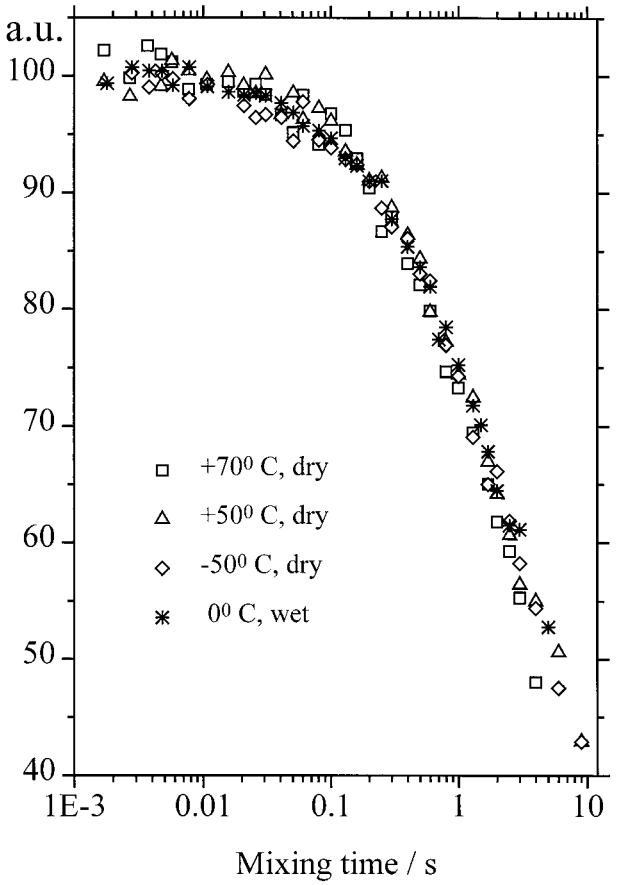

FIG. 6. ^{15}N exchange decays divided by T_1 decays for dry and wet barstar at various temperatures.

assume the same orientation of the CSA tensors in the molecular frame for all nitrogens.

The calculation was done for 88 residues (the first residue nitrogen was not taken into account) using the procedure given in Ref. (*28*). Actually, only the decay of the isotropic line (0-order spinning sideband, $N = 0$) was calculated to be compared with the experiment; however, because of the sum over M in Eq. [1], calculation was done for M running from -3 to $+3$, covering all sidebands of reasonable intensity.

The probabilities $P_{ij}(\tau_m)$ were obtained from the numerical solution of Eq. [2] for the case of the 88-site spin exchange, where k_{ij} were assumed to be in the form of Eq. [9]. Internuclear distances r_{ij} were also obtained from the PDB file of barstar. Then, inserting obtained values of I_{ij}^{MN} and $P_{ij}(\tau_m)$ at different mixing times into Eq. [1], we obtained the spin diffusion exchange decay. Variation of the parameter A (Eq. [9]) results only in compressing or stretching of the exchange decay on the linear τ_m axis.

The simulated curve together with the experimental exchange decays divided by T_1 decays, as described above, are presented in Fig. 8. By varying the parameter A we tried to make the simulated and experimental decays coincide. However, as shown, the shapes of these decays are slightly different, and it is not possible to obtain exact coincidence. We believe that this is primarily the result of the oversimplified assumptions that were made for the calculation: first of all, the identity of the CSA tensor elements for all nitrogens and neglecting the isotropic chemical shift differences between them. Spin diffusion between backbone and sidechain nitrogens was not considered. We also neglected the effects of molecular motion, i.e., we took only the averaged CSA tensor orientations for all nitrogens. In the real protein, the number of sites involved in the SE is substantially greater than 88 because the sites accessible by the MR must also be considered. Taking all this into account would definitely change the shape of the spin diffusion exchange decay.

From the best fitting of the simulated and experimental curves (Fig. 8) we estimated the parameter A (Eq. [9]). It has a value of 100–150 Å^6 s^{-1}. The distance between the neighboring backbone nitrogens in the polypeptide chain is about 3 Å. From this using Eq. [9], it is very easy to estimate that the spin exchange rate between neighboring nitrogens in the protein is about 0.2 s^{-1}.

Spin diffusion between natural-abundance ^{13}C nuclei in poly-

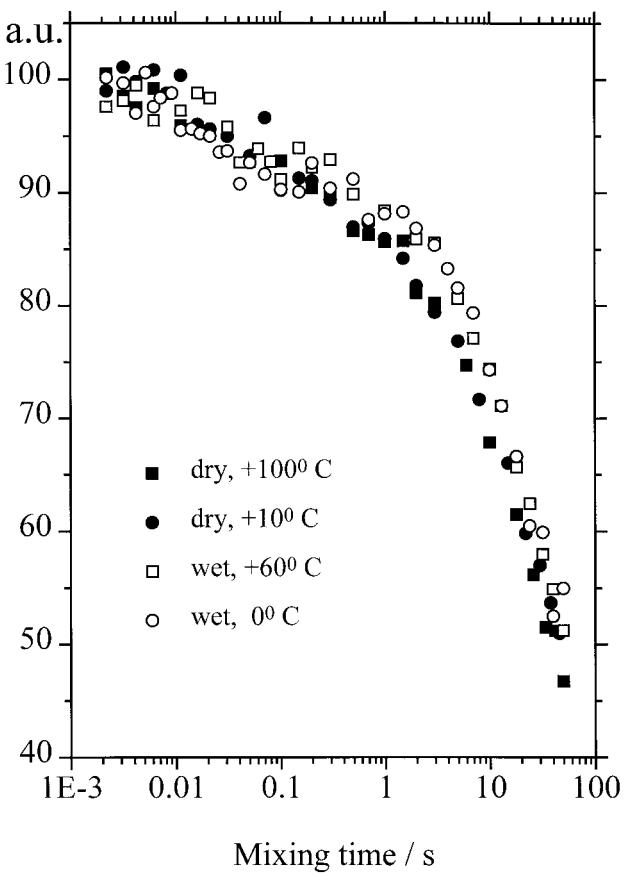

FIG. 7. ^{13}C natural-abundance exchange decays in dry and wet polyglycine.

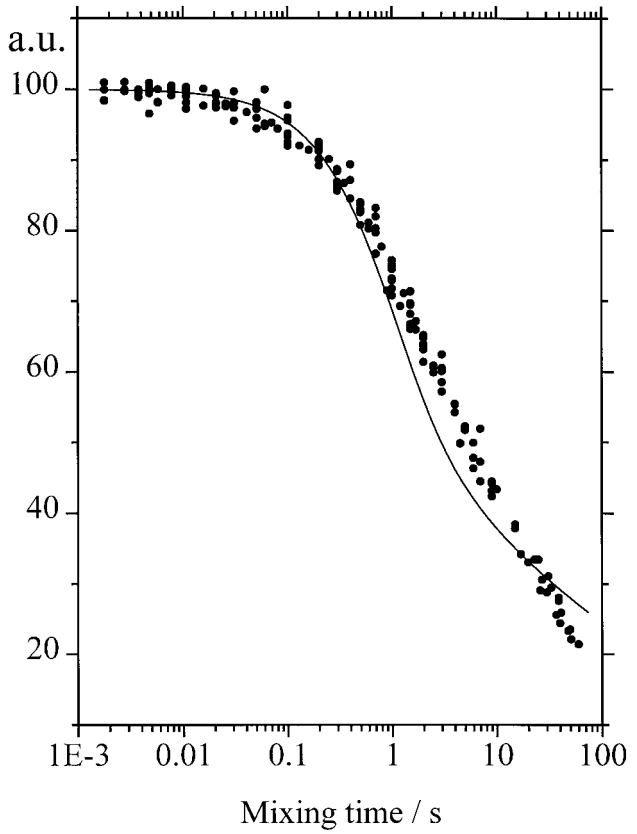

FIG. 8. ^{15}N exchange decays of dry and wet (below 0° C) barstar, divided by T_1 decays (circles). The solid line is the theoretical exchange decay due to the spin diffusion calculated from the known spatial structure of the protein (see details in the text).

glycine has a more complicated picture. Because of the irregular distribution of ^{13}C among ^{12}C nuclei, the distribution of k_{SE} values is much wider than in the ^{15}N case. For the exchange experiment, not only does spin diffusion between carbonyl carbons matter; so does that between carbonyl and any other carbons. First of all, let us estimate the largest k_{SE} value in this distribution. That can be done on the basis of the calculations performed for ^{15}N spin diffusion in barstar. The largest k_{SE} value corresponds to the ^{13}C nuclei pair separated by the shortest possible distance, i.e., the length of one covalent bond, which is about 1 Å. Since k_{SE} is proportional to γ^4/r^6 (*32*), proceeding from the k_{SE} value obtained for the ^{15}N neighbors (see above) one may estimate that the highest k_{SE} value is about 5000 s^{-1}. Such a high value means that the exchange process due to the spin diffusion should be observed in the exchange experiment even at mixing times around 1 ms. Of course, the share of closely spaced ^{13}C nuclei in the total number of ^{13}C pairs is very low, and so is the relative amplitude of the corresponding component of the exchange decay. However, low-amplitude motions give little exchange decays as well; hence, one will have problems in separating them.

On the other hand, we may very roughly estimate the average distance between ^{13}C nuclei from the average value of the carbon density in biopolymers (about 1 atom per 20–50 cubic angstroms) and natural abundance of ^{13}C nuclei (1.1%). These approximate calculations give the average distance between ^{13}C nuclei of the order of 10 Å. Recalling again that k_{SE} is proportional to $1/r^6$, one may estimate that k_{SE} values for natural-abundance ^{13}C nuclei span from 10^{-3}–10^{-2} to 10^3–10^4 s^{-1}. Indeed, in Fig. 7 one may see a slope of the exchange decays starting from the very short mixing times. Absence of the temperature dependence of the initial part of the decays confirms that it is just the spin diffusion.

These rough estimations demonstrate that exchange experiments on natural-abundance ^{13}C nuclei are a rather unsuitable tool for studying low-amplitude molecular motions in organic polymers. Although the existence of the molecular reorientation can be detected qualitatively by temperature variation of the initial part of the exchange decays, correctly obtaining its frequency and amplitude parameters is a very difficult task, since there will be a complex mixture of MR and SE processes in all time scales of the exchange measurements.

Molecular Reorientation

The main goal of the present study is obtaining the information on the superslow backbone motion in our samples. As is clear from the considerations presented above, this information is contained only in the initial part of the exchange decays in the wet barstar at high temperatures (Fig. 5, left). Thus, we need to define the parameters of the shortest component of the exchange decays that is attributed to the MR process. Simple two- or three-exponential decomposition of the exchange decays may lead to a quantitatively wrong result, since the spin diffusion component, as we already know, has a nonexponential form. Besides, one may expect that the MR component also has a nonexponential form, since different domains of the protein globule may have different internal mobility and we are not yet able to separate them in the spectrum.

To extract the MR component we used the following procedure. As seen from Fig. 5, at $T = +50$°C the MR component is significant only at mixing times shorter than 20 ms, whereas at longer mixing times, the shape of the exchange decay is defined mainly by SE process. This can be concluded from the existence of the quasi-plateau that is observed between 20- and 100-ms mixing times at this temperature. This plateau means that the MR component has already decayed and the SE component merely starts to decay at these mixing times. Then, we approximated the exchange decay at $T = +50$°C from 20 ms to 8 s by a biexponential function and extrapolated this function to the shorter mixing times. In this way we obtained the SE component that is shown by the solid line in the left plot of Fig. 5.

Of course, this procedure is somewhat arbitrary. The more correct way to obtain the SE component would be to measure the exchange decays at higher temperatures so that the MR

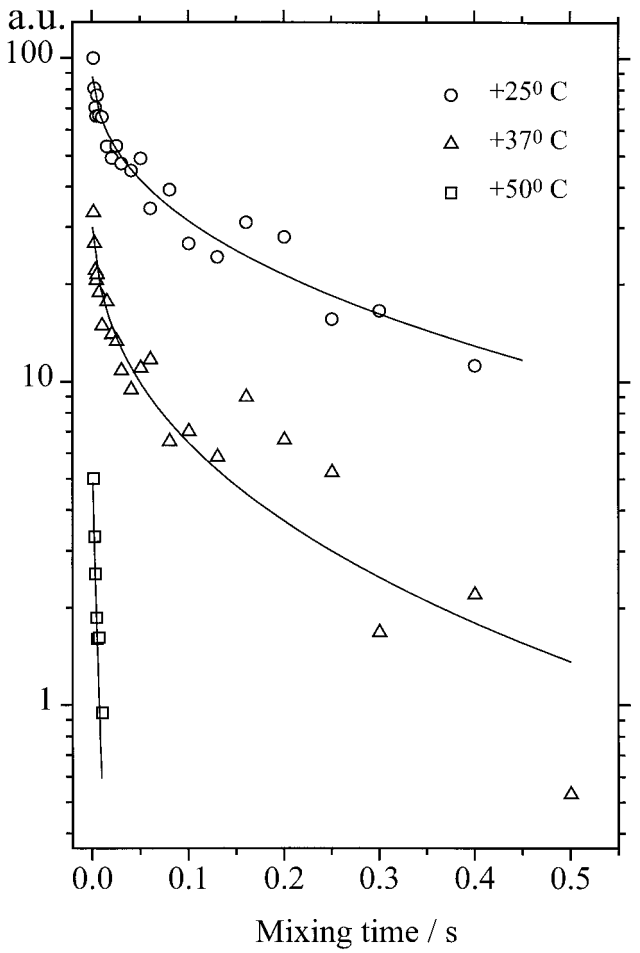

FIG. 9. MR component of the exchange decays in wet barstar at +25, +37, and +50°C. The solid lines are the stretched exponential fitting curves.

component would be too short to be seen in the experiment at all. We tried to perform the experiments at +65 and +80°C; however, after that the results at lower temperatures were not reproducible (whereas after heating up to +50°C the reproducibility was good). This most probably means that at high temperatures the protein was denatured. Thus, we extracted the SE component from the +50°C exchange decay as described previously. We believe that for the first approximation analysis of the exchange data this is a suitable assumption.

After the SE component was obtained, it was subtracted from the exchange decays at $T = +50, +37$, and +25°C. The MR component obtained in this way is shown in Fig. 9. As expected, the decays obviously have a nonexponential form. For the quantitative analysis the decays were approximated using the so-called stretched exponential function

$$A(\tau_m) = \exp(-(\tau_m/\tau_{MR})^{\beta}), \qquad [10]$$

where τ_{MR} is the correlation time of the molecular reorientation, and β is the phenomenological distribution width parameter varying from 0 to 1. (The less β, the wider the distribution of the correlation times.) From fitting the MR components, we obtained τ_m and β for three temperatures. The temperature dependence of τ_m and the activation energy of the MR process are shown in Fig. 10. As for the parameter β, it was found to be 0.4 ± 0.2 at temperatures +25 and +37°C. At $T = +50$°C, it was practically undefined because of the lack of experimental points in the decay.

Another important parameter of the MR process is the relative amplitude of the MR component of the exchange decay. Its value in wet barstar was found to be 0.13 (Fig. 5, left). As mentioned above, the parameter P_{ex1} (Eq. [8]) is a measure of the amplitude of molecular motion. Though the exact molecular model of the slow motion in the protein is not known, from P_{ex1} one may estimate the minimal angle amplitude of this motion using the simplest two-site model. This model assumes that the chemical shift tensor can accept only two equal population orientations (sites). Then the relative amplitude of the exchange component of the decay can be obtained using Eq. [5] or [8]. Values of the tensor elements σ_{xx}, σ_{yy}, σ_{zz} of backbone nitrogens were given above. The three Euler angles that are necessary for computing I_{11} and I_{12} cannot be defined from one experimental parameter P_{ex}; however, the minimal possible angle amplitude can be estimated if we assume that two sites are the result of the rotation of the tensor around its

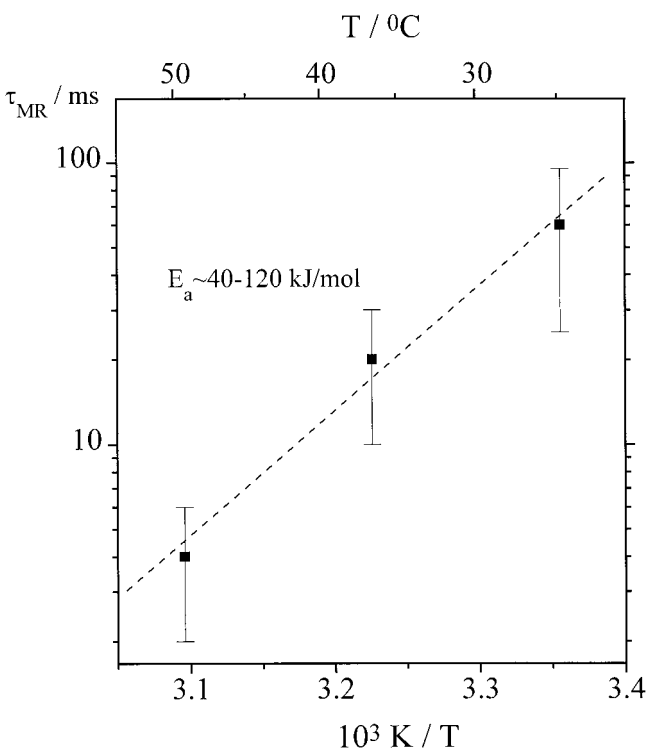

FIG. 10. Temperature dependence of the correlation time of the MR component. Dashed line is the best-fit Arrhenius dependence.

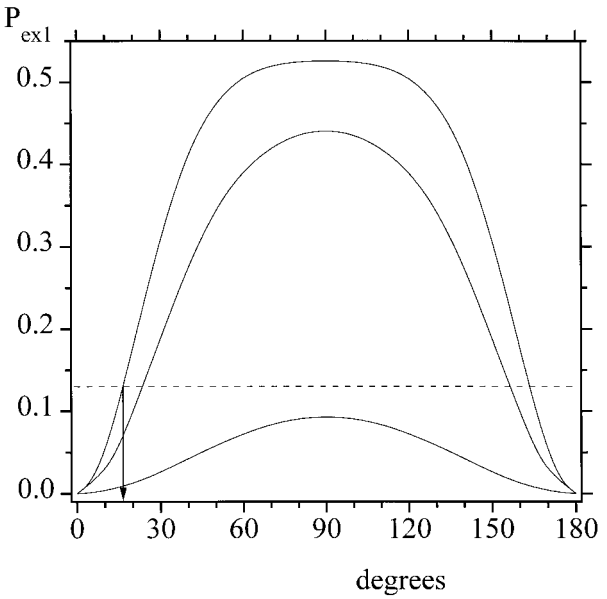

FIG. 11. Relative amplitude of the MR component as a function of the angle of chemical shift tensor rotation around an axis for the two-site model (Eqs. [5] and [8]) for ^{15}N experiments. Three curves correspond to rotation around the shortest (upper), intermediate (middle), and longest (lower) axes. Dashed line corresponds to the experimental value of P_{ex1}. The minimum possible amplitude for the two-site model is marked by an arrow.

shortest (in absolute value) axis. In this case the two longest axes, having opposite signs, change their orientation. In this way the chemical shift of the nuclei is being changed in most effective way, and thus a minimum angle transformation of the tensor is required to achieve the experimental value of P_{ex1}. The same P_{ex1} can be obtained from other kinds of tensor transformations, including shortest axis reorientation, but the angle amplitude in this case should be obviously higher to achieve the same value of P_{ex1}. This is illustrated in Fig. 11, where P_{ex} is represented as a function of the angle of chemical shift tensor rotation around three axes for the two-site model. Assuming rotation around the shortest axis and taking the experimental value of P_{ex1}, we estimated the minimal angle amplitude of the motion. The result is 17° (Fig. 11). Note that this value is the averaged one and some parts of the protein backbone may have even higher amplitudes.

The detected slow correlation time and the relatively high angular amplitude and activation energy of the slow motion suggest that we observed infrequent large amplitude jumps between different protein subconformations rather than oscillations within one energy minimum. It is important that the motion observed in the wet protein is not seen in dry protein and polyglycine, which reveals specificity of this motion to the structure of the biopolymer and humidity level. All the characteristics of the backbone motion obtained above look very similar to the parameters of the slow protein dynamics that have been observed earlier by means of hydrogen exchange or aromatic ring-flip methods in solution (*15*). However, the advantage of the solid-state exchange method is that it enables one to observe the molecular reorientations directly and to define both its frequency and its amplitude parameters.

On the other hand, we must certainly admit that the data obtained in the present work are not yet enough to allow definite and cogent conclusions about molecular models of the slow motion. That will be possible, we believe, in future studies on selectively labeled proteins. This would enable separate characterization of different domains of the protein globule, and in addition less abundant nuclei would make spin diffusion effects negligible, significantly increasing the range of the correlation times of the molecular reorientation that can be observed in the experiment. Our results demonstrate that the application of solid-state MAS exchange spectroscopy is definitely a step forward in investigation of slow protein dynamics on a more detailed molecular level.

CONCLUSIONS

This work has primarily methodology significance. For the first time, solid-state MAS exchange NMR spectroscopy was applied to studying superslow biopolymer dynamics, and as a result, the molecular motion of the protein backbone in the millisecond range of correlation times was detected. It was demonstrated that, since spin diffusion can significantly preclude obtaining information on molecular dynamics, special care should be taken for optimal choice of the time scale and temperature ranges of the exchange experiments. It was shown that the molecular motion has a specificity to the type of the polypeptide structure and humidity level that indirectly indicates the biological relevance of this motion. Most probably, this is the type of protein conformational dynamics that has been observed before by chemical exchange methods in solution. However, unlike these methods, the solid-state exchange experiment enables direct investigation of frequency and amplitude parameters of the molecular dynamics. We hope that future studies using this method will bring a deeper understanding of the nature and properties of the slow dynamics and its role in the biological function of proteins.

ACKNOWLEDGMENTS

This work was supported by the Russian Foundation for Basic Research (grant No. 96-04-00106), the Deutsche Forschungsgemeinschaft DFG (grant No. RE 1025/5-1), and the Fonds der Chemischen Industrie. We thank Professors A. Arsenjev and M. Kirpichnikov for their cooperation in preparing the ^{15}N-labeled protein and useful discussions.

REFERENCES

1. A. Bax, S. W. Sparks, and D. A. Torchia, Detection of insensitive nuclei, *Methods Enzymol.* **176,** 134–150 (1989).
2. G. M. Clore, P. C. Driscoll, P. T. Wingfield, and A. M. Gronenborn,

Analysis of the backbone dynamics of interleukin-1 beta using two-dimensional inverse detected heteronuclear ^{15}N–^{1}H NMR spectroscopy, *Biochemistry* **29,** 7387–7401 (1990).

3. J. Engelke, and H. Rueterjans, Backbone dynamics of proteins derived from carbonyl carbon relaxation times at 500, 600 and 800 MHz: Application to ribonuclease T1, *J. Biomol. NMR* **9,** 63–78 (1997).
4. D. Fushman, S. Cahill, and D. Cowburn, The main-chain dynamics of the dynamin pleckstrin homology (PH) domain in solution: Analysis of ^{15}N relaxation with monomer–dimer equilibration, *J. Mol. Biol.* **266,** 173–194 (1997).
5. B. Brutscher, R. Brueschweiler, and R. R. Ernst, Backbone dynamics and structural characterization of the partially folded A state of ubiquitin by ^{1}H, ^{13}C, and ^{15}N nuclear magnetic resonance spectroscopy. *Biochemistry* **36,** 13043–13053 (1997).
6. R. Gaspar Jr., E. R. Andrew, D. J. Bryant, and E. M. Cashell, Dipolar relaxation and slow molecular motions in solid proteins, *Chem. Phys. Lett.* **86,** 327–330 (1982).
7. E. R. Andrew, D. N. Bone, D. J. Bryant, E. M. Cashell, R. Gaspar, Jr., and Q. A. Meng, Proton relaxation studies of dynamics of proteins in the solid state, *Pure Appl. Chem.* **54,** 585–594 (1982).
8. H. B. R. Cole, and D. A. Torchia, An NMR study of the backbone dynamics of staphylococcal nuclease in the crystalline state, *Chem. Phys.* **158,** 271–282 (1991).
9. V. D. Fedotov, N. P. Obuchov, R. A. Zadikhanov, J. Spevacek, and J. Straka, ^{1}H and ^{13}C nuclear magnetic relaxation and local dynamics of lysozyme and synthetic polypeptides, *Appl. Magn. Reson.* **4,** 491–511 (1993).
10. A. Tamura, M. Matsushita, A. Naito, S. Kojima, K.-I. Miura, and K. Akasaka, Dynamics of the three methionyl side chains of *Streptomyces* subtilisin inhibitor: Deuterium NMR studies in solution and in the solid state, *Protein Science* **5,** 127–139 (1996).
11. A. G. Krushelnitsky, V. D. Fedotov, J. Spevacek, and J. Straka, Dynamic structure of proteins in solid state. ^{1}H and ^{13}C NMR relaxation study, *J. Biomol. Struc. Dynam.* **14,** 211–224 (1996).
12. A. M. Gil, K. Masui, A. Naito, A. S. Tatham, P. S. Belton, and H. Saito, A ^{13}C-NMR study on the conformational and dynamical properties of a cereal seed storage protein, C-hordein, and its model peptides, *Biopolymers* **41,** 289–300 (1997).
13. K. Schmidt-Rohr and H. W. Spiess, "Multidimensional Solid-State NMR and Polymers," Academic Press, London (1994).
14. K.-B. Wong, A.R. Fersht, and S.M.V. Freund, NMR ^{15}N relaxation and structural studies reveal slow conformational exchange in barstar C40/82A, *J. Mol. Biol.* **268,** 494–511 (1997).
15. L. J. Smith, and C. M. Dobson, NMR and protein dynamics, *Int. J. Quant. Chem.* **59,** 315–332 (1996).
16. N. A. Farrow, O. Zhang, J. D. Forman-Kay, and L. E. Kay, A heteronuclear correlation experiment for simultaneous determination of ^{15}N longitudinal decay and chemical exchange rates of systems in slow equilibrium, *J. Biomol. NMR* **4,** 727–734 (1994).
17. M. Akke, J. Liu, J. Cavanagh, H. P. Erickson, and A. G. Palmer, Pervasive conformational fluctuations on microsecond time scales in a fibronectin type III domain, *Nat. Struct. Biol.* **5,** 55–59 (1998).
18. R. Ishima, P. T. Wingfield, S. J. Stahl, J. D. Kaufmann, and D. A. Torchia, Using amide ^{1}H and ^{15}N transverse relaxation to detect millisecond time-scale motions in perdeuterated proteins: Application to HIV-1 protease, *J. Am. Chem. Soc.* **120,** 10534–10542 (1998).
19. D. Reichert, H. Zimmermann, T. P. Tekely, R. Poupko, and Z. Luz, Time-reverse ODESSA. A 1D exchange experiment for rotating solids with several groups of equivalent nuclei, *J. Magn. Reson.* **125,** 245–258 (1997).
20. R. W. Hartley, Barnase and barstar: two small proteins to fold and fit together, *Trends Biochem. Sci.* **14,** 450–454 (1989).
21. G. Schreiber, and A. R. Fersht, Interaction of barnase with its polypeptide inhibitor barstar studied by protein engineering, *Biochemistry* **32,** 5145–5150 (1993).
22. D. N. M. Jones, M. Bycroft, M. J. Lubienski, and A. R. Fersht, Identification of the barstar binding site of barnase by NMR spectroscopy and hydrogen–deuterium exchange, *FEBS Lett.* **331,** 165–172 (1993).
23. M. J. Lubienski, M. Bycroft, S. Freund, and A. R. Fersht, Three-dimensional solution structure and ^{13}C assignments of barstar using nuclear magnetic resonance spectroscopy, *Biochemistry* **33,** 8866–8877 (1994).
24. F. M. Studier, and B. A. Moffatt, Use of bacteriophage T7 RNA polymerase to direct selective high-level expression of cloned genes, *J. Mol. Biol.* **189,** 113–130 (1986).
25. F. M. Studier, A. H. Rosenberg, J. J. Dann, and J. W. Dubendorff, Use of T7 RNA polymerase to direct expression of cloned genes, *Methods Enzymol.* **185,** 60–89 (1990).
26. A. A. Schulga, F. T. Kurbanov, B. Ranjbar, I. I. Protasevich, A. A. Makarov, and M. P. Kirpichnikov, Mapping of functionally and structurally important regions in bacterial ribonucleases: study of himeric barnase/binase proteins, *in* "Proceedings, the 4th International Meeting Ribonucleases: Chemistry, Biology, Biotechnology, 1996, The Netherlands," p. S1P14.
27. J. Sambrook, E. F. Fritsch, and T. Maniatis, "Molecular Cloning: A Laboratory Manual," Cold Spring Harbor Laboratory Press, New York (1989).
28. Z. Luz, H. W. Spiess, and J. J. Titman, Rotor synchronized MAS two-dimensional exchange NMR in solids. Principles and applications, *Isr. J. Chem.* **32,** 145–160 (1992).
29. D. A. Torchia, The measurement of proton-enhanced carbon-13 T_1 values by a method which suppresses artifacts, *J. Magn. Reson* **30,** 613–616 (1978).
30. R. R. Ernst, G. Bodenhausen, and A. Wokaun, "Principles of Nuclear Magnetic Resonance in One and Two Dimensions," Chap. 9, Clarendon Press, Oxford (1987).
31. G. Lipari and A. Szabo, Model-free approach to the interpretation of nuclear magnetic resonance relaxation in macromolecules, *J. Amer. Chem. Soc.* **104,** 4546–4559 (1982).
32. Z. Olender, D. Reichert, A. Muller, H. Zimmermann, R. Poupko, and Z. Luz, Carbon-13 chemical-shift correlation, spin diffusion and self diffusion in isotopically enriched tropolone, *J. Magn. Reson.* **A120,** 31–45 (1996).
33. D. Reichert, G. Hempel, R. Poupko, Z. Luz, Z. Olejniczak and P. Tekely, Carbon-13 spin exchange in durene as studied by MAS NMR spectroscopy, *Sol. State Nucl. Magn. Reson.* **13,** 137–148 (1998) .
34. J. Herzfeld and A. Berger, Sideband intensities in NMR spectra of samples spinning at the magic angle, *J. Chem. Phys.* **73,** 6021–6030 (1980).
35. Y. Hiyama, C.-H. Niu, J. V. Silverton, A. Bavoso, and D. A. Torchia, Determination of ^{15}N chemical shift tensor via ^{15}N–^{2}H dipolar coupling in boc-glycylglycyl[^{15}N]glycine benzyl ester, *J. Amer. Chem. Soc.* **110,** 2378–2383 (1988).